

Overlaying optical lattices for simulation of complex frustrated antiferromagnets

Zhi-Xin Chen¹, Han Ma², Mo-Han Chen¹, Xiang-Fa Zhou¹, Lixin He¹,
Guang-Can Guo¹, Xingxiang Zhou^{1,*}, Yan Chen^{2,†} and Zheng-Wei Zhou^{1,‡}

¹*Key Laboratory of Quantum Information, University of Science and
Technology of China, Hefei, Anhui 230026, China*

²*Department of Physics, State Key Laboratory of Surface Physics,
Laboratory of Advanced Materials and Key Laboratory of Micro and Nano Photonic
Structures (Ministry of Education), Fudan University, Shanghai, 200433, China*

We present design techniques of special optical lattices that allow quantum simulation of spin frustration in two-dimensional systems. By carefully overlaying optical lattices with different periods and orientations, we are able to adjust the ratio between the nearest-neighbor and next-nearest-neighbor interaction strengths in a square spin lattice and realize frustration effects. We show that only laser beams of a single frequency is required, and the parameter space reachable in our design is broad enough to study the important phases in the J_1 - J_2 frustrated Heisenberg model and checkerboard antiferromagnet model. By using the polarization spectroscopy for detection, distinct quantum phases and quantum phase transition points can be characterized straightforwardly. Our design thus offers a suitable setup for simulation of frustrated spin systems.

PACS numbers: 67.85.-d, 37.10.Jk, 05.30.Fk

I. INTRODUCTION

Geometrically frustrated systems with strong correlation have attracted much attention due to the highly nontrivial interplay between frustration and correlation [1, 2]. In such systems, not all pairs of spins can simultaneously assume their lowest energy configuration, and the ground state usually has a large number of degeneracies. In particular, frustration in quantum antiferromagnets may cause certain types of magnetically disordered quantum phases, including the resonating valence bond spin liquid state [3] and the valence bond crystal state [4]. As an exotic state of quantum matter, the spin liquid in quantum frustrated antiferromagnets is a topic of great interest in condensed matter physics. In such states, the local moments do not form ordering down to the very low temperatures despite of strong antiferromagnetic couplings. It has been proposed that these exotic states are closely related to the mechanism of high- T_c superconductivity [3]. For instance, the quantum spin liquid state could become unconventional superconducting state when the charge carriers are introduced.

Despite intense studies over the past several decades, the nature of spin liquid in the strongly frustrated regime remains poorly understood. A typical system is the frustrated J_1 - J_2 Heisenberg model on a square lattice. Besides the nearest neighboring (nn) spin interactions leading to Néel state, the J_1 - J_2 Heisenberg model contains extra next nearest neighboring (nnn) spin interactions. Frustration may lead to the destruction of long-range order like Néel order, and quantum disordered phases may

show up in the strongly frustrated regime with appreciable value of J_2/J_1 . Many candidates for the ground states have been suggested, such as a columnar spin dimerized state, a plaquette resonating valence bond phase, and a columnar spin dimerized state with plaquette-type modulation. Because of the difficulties in theoretical and experimental studies of the frustrated spin liquid physics, a quantum simulator for such systems is highly valuable [5, 6].

Recent advance in the manipulations of ultracold atoms in optical lattice has opened new possibilities for realizing simulation of many significant strongly correlated quantum models [6, 7]. Much efforts have been devoted to the simulation of quantum magnetism in ultracold lattice gases. Recent experiments have shown the evidences of superexchange interactions between two neighboring sites [8]. Very recently, the realization of large scale quantum simulator of frustrated magnetism in triangular optical lattices has been achieved [9]. As for the simulation of the geometrically frustrated antiferromagnets, an effective manipulating method is highly demanded to reach the strongly frustrated regime of the J_1 - J_2 Heisenberg model where the exotic quantum spin liquid states may appear around $J_1/J_2 \sim 0.5$. However, it is technically difficult to achieve the interesting physical regime. As we know, the amplitude of intersite tunneling rate decreases exponentially with their distance and thus the nnn tunneling rate is much smaller than the nn tunneling rate in a normal square lattice. According to the mechanism of superexchange interactions, the value of J_2/J_1 is much more suppressed.

Another outstanding difficulty in exploring magnetic systems in cold atoms is the detection of quantum many-body states. Various detection methods have been proposed during the past years. The noise correlations techniques [10, 11] may detect density-density correlations, which corresponds to the spin-spin correlations. Anal-

*Electronic address: xizhou@ustc.edu.cn

†Electronic address: yanchen99@fudan.edu.cn

‡Electronic address: zwzhou@ustc.edu.cn

ogous to the neutron diffraction in condensed matter systems, Bragg scattering spectroscopy [12] may probe the static spin structure factor of the Néel state. Single-lattice detectors [13] may measure magnetic ordering, but is still a kind of destructive technique. Recently, the polarization spectroscopy technology [14] was proposed to detect magnetic correlations including ferromagnetic and antiferromagnetic but also more exotic spin ordering by tuning the parameters of polarized light, which makes it a valuable tool for quantum states measurement.

Engineering of optical lattices has proven very versatile as shown in previous studies [15, 16] where suitable laser beam configurations have been employed to produce sophisticated optical lattices. In this work, we push the idea further by overlaying optical lattices with different periods and orientations to realize spin frustration effects in two-dimensional square lattices. Filling such a carefully designed optical lattice with ultracold fermionic atoms, we can then manipulate spin-spin exchange interaction between two next-nearest neighboring atoms in optical lattice by adjusting the optical potentials. We calculate the tunneling rate in the square lattice and find that the nnn tunneling rate could be comparable to the nn tunneling rate. It turns out that the J_1 - J_2 Heisenberg model in the strongly frustrated regime could be realized in which the exotic spin liquid states may exist. Moreover, we can simulate other geometrically frustrated lattice like the checkerboard antiferromagnet model. As for the detection of quantum many-body states, we utilize the polarization spectroscopy technology [14] to study the spatially resolved spin-spin correlation functions. For J_1 - J_2 Heisenberg model, we demonstrate that this promising method can be used to determine the quantum phase transition points straightforwardly and characterize distinct quantum phases. In particular, one-to-one correspondence between the extreme points of noise signal and quantum phase transition points has been achieved.

The rest of the paper is organized as follows. In Sec. II, we implement the two-dimensional frustrated optical lattice using a special optical engineering technique. In Sec. III, simulations of the J_1 - J_2 Heisenberg model and the checkerboard antiferromagnet model are introduced. In Sec. IV, we employ the polarization spectroscopy technology to detect the quantum many-body states. Finally Sec. V gives a summary.

II. THE TWO-DIMENSIONAL FRUSTRATED OPTICAL LATTICE

The Heisenberg spin interactions between neighboring ultracold atoms in an optical lattice arise due to the intersite virtual tunneling of atoms [16, 17]. Consequently, the spin-spin exchange interaction depends on the intersite tunneling rate t as well as the on-site Coulomb interaction U via the superexchange mechanism, $J \sim t^2/U$. To implement a J_1 - J_2 Heisenberg model in the strongly

frustrated regime, the crucial procedure is to design a special two-dimensional optical lattice in which the nn tunneling rate t_2 can be comparable to or even larger than the nn tunneling rate t_1 . It is hard to achieve by creating ordinary optical lattices using laser beams of the same wave number k as is required to trap atoms in a certain state. However, by properly designing several optical lattices with laser beams traveling in different directions and superimposing them elaborately, we can tune the effective potential barriers along different directions and realize such a frustrated optical lattice using laser beams with the same wave number k .

We start by creating a normal two-dimensional square lattice. First, we use a strong standing-wave field in the z direction to completely suppress the tunneling of atoms along the z direction. Then, as shown in Fig. 1(a), we shine a pair of blue-detuned interfering traveling laser beams of wave number k in the z - x plane, each with an angle of $\pi/4$ with respect to the x - y plane. These two laser beams co-propagate in the z direction and counter-propagate in the x direction. Together with the strong trapping field in the z direction, it creates a periodic potential along the x direction in the x - y plane. Similarly, as shown in Fig. 1(a), we shine one more pair of blue-detuned interfering laser beams in the y - z plane, each with an angle of $\pi/4$ with respect to the x - y plane. This creates a periodic potential along the y direction in the x - y plane. The net effect of these trapping lasers is the formation of the following two-dimensional spatially varying potential profile:

$$V_1(x, y) = V_1 \left[\sin^2 \left(\frac{k}{\sqrt{2}} x + \frac{\pi}{2} \right) + \sin^2 \left(\frac{k}{\sqrt{2}} y + \frac{\pi}{2} \right) \right], \quad (1)$$

where k is the wave vector for the laser beams and V_1 is proportional to the dynamical atomic polarizability times the laser intensity. Its projection into the x - y plane is $k/\sqrt{2}$. This potential profile then produces a square optical lattice with a period $a_1 = \lambda/\sqrt{2}$ where the wavelength $\lambda = 2\pi/k$. We load the optical lattice such that there is one atom trapped at each minimum of the optical potential. In such an optical lattice, since the tunneling rate is sensitive to the potential barrier height and lattice site separation, it can be easily seen from Fig. 1(b) that the nnn tunneling rate along the diagonal direction is much smaller than the nn tunneling along the x , y directions. This is because the potential barrier along the diagonal direction is higher and the distance between the sites in that direction is also larger.

In order to make the nnn tunneling rate t_2 comparable to the nn tunneling rate t_1 and thus realize an appreciable J_2/J_1 , we must adjust the potential barrier heights along both the diagonal and x , y directions. For this purpose, we add another square lattice along the diagonal direction in the x - y plane with a lattice period $a_2 = \lambda/2$. As shown in Fig. 1(c), this second lattice can be created by applying two pairs of standing-wave laser beams in the x - y plane along the diagonal directions and of the same wave number k as those used earlier to engineer the po-

tential profile in Eq. (1). Its lattice potential has the form

$$V_2(x, y) = V_2 \left[\sin^2 \left(\frac{k}{\sqrt{2}}(x + y) \right) + \sin^2 \left(\frac{k}{\sqrt{2}}(x - y) \right) \right]. \quad (2)$$

To avoid undesired interferences between laser beams, one can randomize the relative orientation of the polarization of laser beams generating optical lattice potentials of V_1 and V_2 [15]. Thus, the total effective two-dimensional optical potential is a sum of $V_1(x, y)$ and $V_2(x, y)$. Its profile is plotted in Fig. 1(d) for $V_1 = 10E_R$ and $V_2 = 15E_R$ where $E_R = \hbar^2 k^2 / 2m$ is the atomic recoil energy. The corresponding lattice configuration is depicted in Fig. 1(e). It is clear that due to the second lattice we engineered, the effective potential barriers along x, y directions are much enhanced and the tunneling between nearest neighbors is suppressed. In contrast, the effective potential barrier along the diagonal direction is lowered and the tunneling between nnn is enhanced. Thus, we can tune the ratio t_2/t_1 by adjusting the value of V_2/V_1 .

To find out more practical parameter region of t_2/t_1 in a physical system, we numerically calculate these tunneling rates for an optical lattice loaded with Sodium atoms. The tunneling rate between site i and site j is shown as,

$$t_{ij} = \langle W_i | H_0 | W_j \rangle, \quad (3)$$

where $|W_i\rangle, |W_j\rangle$ are the Wannier functions [18, 19] at sites i and j , and $H_0 = -\nabla^2/2 + V_1(x, y) + V_2(x, y)$ denotes the single-particle Hamiltonian of the system. Here we consider the lowest band only. For the Sodium atoms, $E_R/\hbar = 2\pi \times 32$ kHz for a blue detuned $\lambda = 514$ nm. We may choose $V_1 = 10E_R$ and increase V_2 from 0 to $20E_R$ and then plot t_1 and t_2 in Fig. 1(f). It is obvious that the value of t_2 (t_1) increases (decreases) as V_2 increases. Notably, t_2 becomes larger than t_1 when $V_2 > 15E_R$. Therefore, by using a sufficiently large V_2 , we can simulate the J_1 - J_2 Heisenberg model in the strongly frustrated regime. It is worth to mention that we have shown theoretically the way to simulate an one-dimensional J_1 - J_2 model in concatenated microcavities [20]. However, it is quite difficult to realize a two-dimensional J_1 - J_2 model in the strongly frustrated regime by employing this method.

Moreover, we can realize a checkerboard lattice by adding a third square lattice with a lattice period $a_3 = \lambda$ along the diagonal direction in the x - y plane. Since the period of this third lattice is twice of the second lattice and both are oriented in the same direction, the diagonal tunnelings in half of the lattice are strongly suppressed due to the presence of potential maxima, and a checkerboard lattice can be constructed. To generate the third lattice, we may adopt a technique similar to that used for the first simple lattice. In Fig. 2(a), m is one diagonal direction in the x - y plane and m' is the other diagonal direction perpendicular to m . We shine a pair of blue-detuned interfering traveling laser beams of wave number k in the m - z plane, each with an angle $\pi/3$ with respect

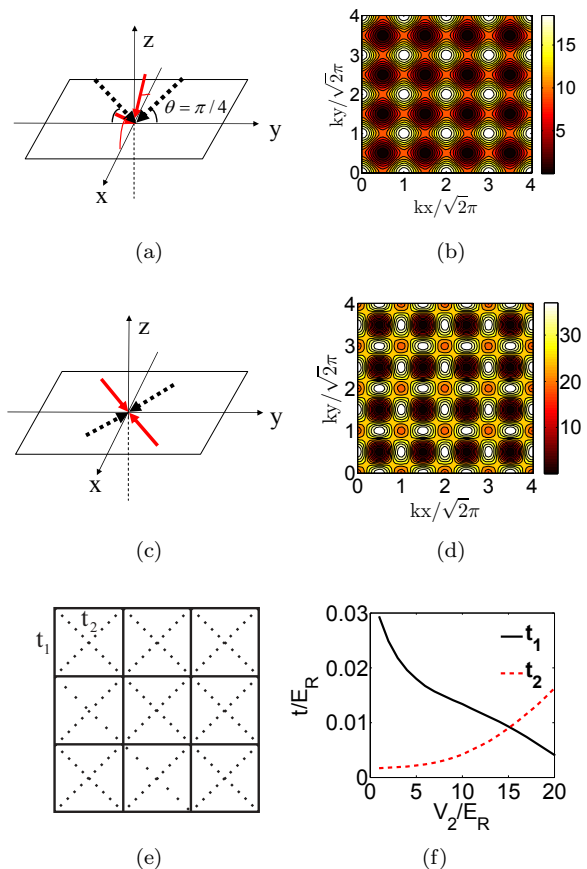


FIG. 1: (Color online) (a) Schematic diagram for generating the interference field $V_1(x, y)$. (b) Normal square lattice pattern induced by the field $V_1(x, y)$ in unit of E_R . (c) Schematic diagram for generating the interference field $V_2(x, y)$. (d) The square lattice pattern induced by the field $V_1(x, y) + V_2(x, y)$ in unit of E_R . (e) Schematic diagram of the square lattice with diagonal tunneling. (f) The nearest-neighboring tunneling t_1 (black solid line) and the next-nearest-neighboring tunneling t_2 (red dashed line) as a function of V_2 in unit of E_R .

to the x - y plane. Similarly, another pair of blue-detuned traveling laser beams of the same wave number are shot in the m' - z plane, each with an angle $\pi/3$ with respect to the x - y plane. Obviously, these two pairs of laser beams will form a two-dimensional lattice along the diagonal directions in the x - y plane and its period is determined by the projected wave number in the x - y plane $k'_{\parallel} = k/2$. Specifically, the spatially varying potential profile for the third lattice is

$$V_3(x, y) = V_3 \left[\sin^2 \left(\frac{\sqrt{2}}{4} k(x + y) \right) + \sin^2 \left(\frac{\sqrt{2}}{4} k(x - y) \right) \right]. \quad (4)$$

For amplitudes $V_1 = 10E_R$, $V_2 = 10E_R$ and $V_3 = 5E_R$, the superposed potential $V(x, y) = V_1(x, y) + V_2(x, y) + V_3(x, y)$ is plotted in Fig. 2(b). We can see that there are two sets of plaquettes in which the potential barrier heights along the diagonal direction are raised and low-

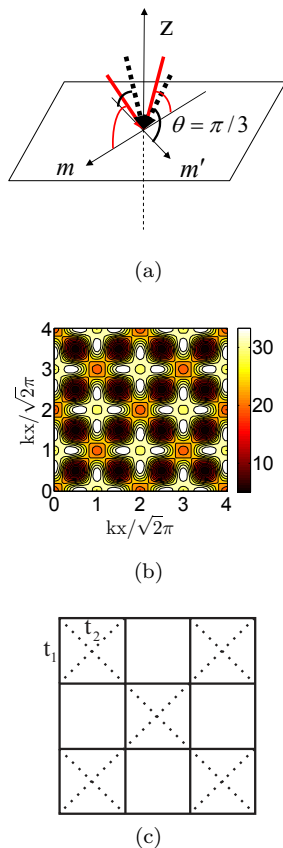


FIG. 2: (Color online) (a) Schematic diagram for generating the interference field $V_3(x, y)$. (b) The optical lattice induced by interference field $V(x, y)$ in unit of E_R . (c) Schematic diagram of a checkerboard lattice.

ered respectively. Consequently, the diagonal tunnelings in these two sets of plaquettes are either suppressed or enhanced, providing us the checkerboard lattice. The configuration of the checkerboard lattice is shown in Fig. 2(c). When we fix the value of V_1 and V_3 and adjust the value of V_2 , the rate of t_2/t_1 will be changed accordingly. When t_2 is comparable to t_1 , the checkerboard J_1 - J_2 model may reach the strongly frustrated regime $J_2/J_1 \sim 1$.

III. THE FRUSTRATED J_1 - J_2 HEISENBERG MODELS

We can implement the J_1 - J_2 Heisenberg model by using a collection of ultracold fermionic atoms confined in the special square optical lattice at integer filling. In the real experiments, ultracold fermionic atoms have been used to realize the Mott insulating state [21, 22]. By further lowering the temperatures, two easily accessible hyperfine states in such system can be used to realize magnetic orders [23, 24]. Here we consider that the system enters into the Mott insulating state, and then load

the ultracold fermionic atoms onto the optical lattice so that there is only one atom per lattice site. The two hyperfine states represent the effective spin states $|\sigma\rangle = |\uparrow\rangle$ and $|\downarrow\rangle$. We assume that the optical potential has no state dependence and the atoms are confined to the lowest Bloch band. The model Hamiltonian can be written as,

$$H = -t_1 \sum_{\langle i,j \rangle \sigma} (c_{i\sigma}^\dagger c_{j\sigma} + h.c.) - t_2 \sum_{\langle\langle i,j \rangle\rangle \sigma} (c_{i\sigma}^\dagger c_{j\sigma} + h.c.) + U \sum_i n_{i\uparrow} n_{i\downarrow}, \quad (5)$$

where $c_{i\sigma}$ is the Fermion annihilation operator for the atom on site i , $n_{i\sigma} = c_{i\sigma}^\dagger c_{i\sigma}$, t_1 and t_2 are respectively the tunneling matrix elements between two nn sites $\langle i, j \rangle$ and two nnn sites $\langle\langle i, j \rangle\rangle$, and U denotes the on-site repulsive interaction between the atoms. The interaction U can be adjusted by Feshbach resonances method. In the Mott insulator regime, we have $t_1, t_2 \ll U$. By treating the tunneling as weak perturbation and using the Schrieffer-Wolff transformation, it can be shown that Eq. (5) is equivalent to the following J_1 - J_2 Heisenberg model Hamiltonian,

$$H = J_1 \sum_{\langle i,j \rangle} S_i \cdot S_j + J_2 \sum_{\langle\langle i,j \rangle\rangle} S_i \cdot S_j. \quad (6)$$

where $J_i = 4t_i^2/U$ ($i=1,2$), J_1 and J_2 correspond to the nn and nnn exchange couplings, respectively. (see Fig.1c) Here we ignore the higher order corrections for the coefficient J_i , in which the dominant item is proportional to t_i^4/U^3 [25] and can be suppressed greatly as U/t_i grows.

Due to the competition between J_1 and J_2 , the frustrated J_1 - J_2 antiferromagnet has certain limiting cases. At $J_2/J_1 \ll 1$, the model is reduced to the Heisenberg model on a square lattice. At $J_2/J_1 \sim 1$, the system has a collinear antiferromagnetic quasi-long range order. In the strongly frustrated regime $J_2/J_1 \sim 0.5$, there are several candidates of possible spin liquid states, but there is still lack of general consensus. According to previous analytical and numerical studies [26–28], there might be three quantum critical points around $J_2/J_1 \sim 0.38$, 0.5, and 0.6, respectively. In particular, the simple Néel state corresponds to the parameter region $J_2/J_1 < 0.38$, the simple columnar dimerized spin liquid shows up for $0.38 < J_2/J_1 < 0.5$, the columnar dimerized spin liquid with plaquette type modulation may exist in the parameter region $0.5 < J_2/J_1 < 0.6$, and the collinear state may appear when $J_2/J_1 > 0.6$. As illustrated in Fig. 1d, we observe that t_2/t_1 or J_2/J_1 increases progressively as we increases V_2 . It is clear that the strongly frustrated regime of J_1 - J_2 model can be reached. This model also exhibits rich dynamical behaviors which makes it an ideal testing ground for the study of quantum phase transitions. Once the quantum many-body states could be faithfully probed, our proposed quantum simulator may resolve many outstanding issues.

Another interesting frustrated two-dimensional quantum spin model under our consideration is the checkerboard antiferromagnet. Similar to the case of J_1 - J_2 model, we can simulate the checkerboard antiferromagnet model by using ultracold fermionic atoms confined in the checkerboard optical lattice. The model Hamiltonian contains both the nn couplings J_1 and the nnn diagonal link J_2 . In the limit of $J_2/J_1 \ll 1$, its ground state has the Néel long-range order, whereas it corresponds decoupled Heisenberg chains when $J_2/J_1 \gg 1$. According to previous studies [29, 30], there may exist three distinct quantum phases: the Néel order shows up for $J_2/J_1 < 0.8$, a valence bond crystal in singlet plaquettes may appear when $0.8 < J_2/J_1 < 1.1$, and decoupled Heisenberg spin chains corresponds to the parameter region $J_2/J_1 > 1.1$. The checkerboard antiferromagnet model in the strongly frustrated regime $J_2/J_1 \sim 1$ can be realized experimentally with ultracold atoms in optical lattices.

IV. DETECTING THE QUANTUM MANY-BODY STATES

Besides the preparation of the two-dimensional frustrated spin models in optical lattices, another crucial procedure is to detect faithfully the quantum many-body states in these strongly correlated systems. Among many different experimental methods, one of the significant progresses in this field is the quantum polarization spectroscopy of the atomic ensemble, which is a type of quantum non-demolition detection [14]. After a polarized probe laser traveling through the atomic ensemble, the spin fluctuation and correlation of the atomic system will be mapped on those of light, which can then be efficiently measured using homodyne detection. This method can be used to probe the spatially resolved spin-spin correlation functions and then may distinguish different magnetic quantum phases. Recently, this method has been applied to study the phase diagram of spin-1 bilinear-biquadratic model and appears to be quite successful [31]. In the following, we will employ the quantum polarization spectroscopy method to detect the quantum many-body states of a small-scale J_1 - J_2 model and gain some important insights on distinct quantum phases and quantum phase transition points.

Next we consider a probe standing wave polarized in the x direction characterized by the Stokes operators $\hat{s}_1, \hat{s}_2, \hat{s}_3$. We define a macroscopic Stokes operator $\hat{S}_i = \int \hat{s}_i dt$ and introduce the canonical quadrature operators $\hat{X} = \sqrt{2/N_P} \hat{S}_2$, where N_P is the number of photons. The variance of \hat{X} of the output light contains the atomic spin-spin correlations:

$$\langle (\Delta \hat{X}_{out})^2 \rangle = \frac{1}{2} + \frac{\kappa^2}{FN_A} \sum_{k,l=1} c_k c_l (\langle \hat{S}_z^k \hat{S}_z^l \rangle - \langle \hat{S}_z^k \rangle \langle \hat{S}_z^l \rangle), \quad (7)$$

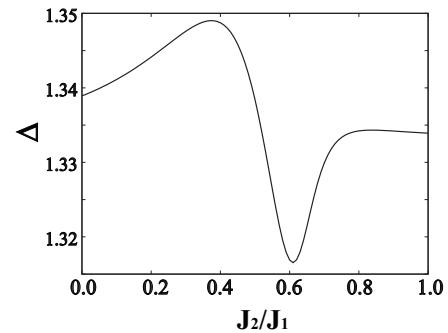


FIG. 3: The noise signal Δ as a function of J_2/J_1 of the J_1 - J_2 frustrated spin model.

where κ is the coupling constant, F is the total angular momentum of a atom, N_A is the total number of atoms, \hat{S}_z^k denotes the z component spin operator of the k th atom. c_n describes the atom-light coupling and is given by

$$c_n(k_p, b) = 2 \int dr \cos^2(k_p(r-b)) |w(r-r_n)|^2, \quad (8)$$

where k_p is the wavevector of the probe laser, b is its shift with the optical lattice and $w(r-r_n)$ is the Wannier wavefunction of the atom confined at site r_n . Here we choose $F = 1/2$ and $\kappa = 1$. The probe laser propagates along the diagonal direction with $k_p = k/4$ and $b = 0$, so the modification of the atom-light coupling c_n has the structure

$$\begin{pmatrix} 2 & 1 & 0 & 1 \\ 1 & 0 & 1 & 2 \\ 0 & 1 & 2 & 1 \\ 1 & 2 & 1 & 0 \end{pmatrix}. \quad (9)$$

The noise signal is defined as $\Delta = \langle (\Delta \hat{X}_{out})^2 \rangle - 1/2$, which is a linear combination of various spatially varying correlation functions. By tuning the parameter like J_2/J_1 of the Hamiltonian, the ground state wavefunction may evolve accordingly. When the tuning parameter crosses the quantum phase transition point, a sudden change of the symmetry of ground state wavefunction may occur. The quantum phase transition may lead to the possible discontinuity of correlation function itself or its first order derivative. We naturally expect that the features of noise signal as a function of parameter should have certain connections with distinct quantum phases and quantum phase transition points. Then we numerically investigate the evolution of Δ as a function of parameter J_2/J_1 of the frustrated spin models and expect to reveal the connections between noise signal and quantum phase transitions.

We numerically calculate the ground state many-body wave function of the spin model by exact diagonalization method for a small cluster [32]. Then we compute the spatially varying spin-spin correlation functions and

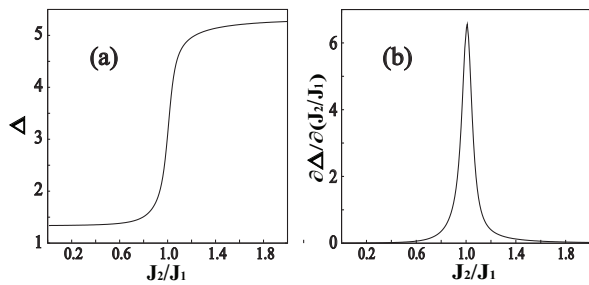


FIG. 4: (a) Δ as a function of J_2/J_1 of the checkerboard antiferromagnet model; (b) Its first derivative versus J_2/J_1 .

finally we obtain the value of the noise signal. For the J_1 - J_2 frustrated model, the noise signal Δ is plotted as a function of J_2/J_1 in Fig. 3. It can be clearly seen that there are two local extreme points at $J_2/J_1 \sim 0.38$ and 0.62 , respectively. By analyzing the first derivative of noise signal Δ as a function of J_2/J_1 , we may locate another extremum point at $J_2/J_1 = 0.5$. According to our natural expectation, we may connect these three extreme points to three possible quantum phase transition points. Very interestingly, these extreme points coincide quite precisely with the known quantum phase transition points (in an infinite system) respectively at $(J_2/J_1)_c = 0.38, 0.5$ and 0.6 [26–28]. This one-to-one correspondence between the extreme points of noise signal and quantum phase transition points is remarkable. According to previous studies, two points at $(J_2/J_1)_c = 0.38$ and 0.6 are connected to the second order quantum phase transition while the point at $(J_2/J_1)_c = 0.5$ may correspond to first order quantum phase transition. That may explain why the two extreme points show up for Δ itself while one extremum point appears for the first derivative of Δ . In view of the small 4×4 cluster used in our calculation, the good agreement of our results with previous studies is truly impressive. In other words, we demonstrate that the polarization spectroscopy method can be used to determine the quantum phase transition points straightforwardly and characterize distinct quantum phases.

For the checkerboard antiferromagnet model, we calculate the noise signal Δ and its first derivative with respect to J_2/J_1 . As shown in Fig. 4, there appears no extreme point for Δ itself, the evolution of Δ as a function of J_2/J_1 can be roughly classified into three different regions, two flatter regions for both $J_2/J_1 < 0.8$ and $J_2/J_1 > 1.2$, and one steeper region for $0.8 < J_2/J_1 < 1.2$. By analyzing the first derivative Δ as a function of J_2/J_1 , there is a clear maximum point around $J_2/J_1 = 1$. From the previous studies [29, 30], there might be three

different phases dividing by two quantum phase transition points which are located at $(J_2/J_1)_c \sim 0.8$ and 1.1 , respectively. In this case, there is no good one-to-one correspondence between the extreme points of noise signal and the quantum phase transition points. Since the unit cell of checkerboard lattice is larger than that of simple square lattice, a larger cluster is required to do numerical calculations. Unfortunately, it is now beyond our computational capabilities.

V. SUMMARY

Simulation of geometrically frustrated quantum antiferromagnets of ultracold fermionic atoms in optical lattices and detection of many-body states become a very hot topic both experimentally and theoretically. In this paper, we have shown such strongly correlated systems can be simulated by a specific optical engineering technique. In particular, both the frustrated J_1 - J_2 Heisenberg model and checkerboard antiferromagnet model in the strongly frustrated regime can be realized for ultracold fermionic atoms in optical lattices. Moreover we employ the polarization spectroscopy method to probe the quantum many-body states of such systems. This method is designed to detect the spatially varying spin-spin correlation functions. In particular, for the J_1 - J_2 model, the quantum phase transition points can be determined straightforwardly and distinct quantum phases can be well characterized. The polarization spectroscopy method is quite promising to probe various magnetic orders of geometrically frustrated systems.

VI. ACKNOWLEDGMENTS

This work was funded by the National Basic Research Program of China (Grants No. 2009CB929204, No. 2012CB921604, and No.2011CB921204), the National Natural Science Foundation of China (Grants No. 11174270, No. 11004186, No. 10874032, No. 10875110, No. 11074043, No. 60836001, and No. 60921091), the Research Fund for the Doctoral Program of Higher Education of China (Grant No. 20103402110024), the Fundamental Research Funds for the Central Universities (Grant No. WK2470000006), and the Shanghai Municipal Government. H.M. is grateful for the support from the Fudan Undergraduate Research Opportunities Program and the National Science Fund for Talent Training in Basic Science. Z.-W.Z. gratefully acknowledges the support of the K. C. Wong Education Foundation, Hong Kong

[1] L. Balents, Nature (London) **464**, 199 (2010).

[2] H.T. Diep, Frustrated Spin Systems (World Scientific

- Publishing Co., Singapore, 2004).
- [3] P. W. Anderson, *Science* **235**, 1196 (1987).
 - [4] N. Read and S. Sachdev, *Phys. Rev. Lett.* **62**, 1694 (1989).
 - [5] S. Lloyd, *Science* **273**, 1073 (1996); I. Buluta and F. Nori, *ibid.* **326**, 108 (2009).
 - [6] I. Bloch, J. Dalibard, and W. Zwerger, *Rev. Mod. Phys.* **80**, 885 (2008).
 - [7] M. Lewenstein, A. Sanpera, V. Ahufinger, B. Damski, A. Sen(de), and U. Sen, *Adv. Phys.* **56**, 243 (2007).
 - [8] S. Trotzky, P. Cheinent, S. Fölling, M. Feld, U. Schnorrberger, A. M. Rey, A. Polkovnikov, E. A. Demler, M. D. Lukin, and I. Bloch, *Science* **319**, 295 (2008).
 - [9] J. Struck, C. Öschlager, R. Le Targat, I. P. Soltan-Panahi, A. Eckardt, M. Lewenstein, P. Windpassinger, and K. Sengstock, e-print arXiv:1103.5944.
 - [10] E. Altman, E. Demler, and M. D. Lukin, *Phys. Rev. A* **70**, 013603 (2004).
 - [11] S. Fölling, S. Trotzky, P. Cheinent, M. Feld, R. Saers, A. Widera, T. Muller, and I. Bloch, *Nature (London)* **448**, 1029 (2007).
 - [12] T. A. Corcovilos, S. K. Baur, J. M. Hitchcock, E. J. Mueller, and R. G. Hulet, *Phys. Rev. A* **81**, 013415 (2010).
 - [13] W. S. Bakr, J. I. Gillen, A. Peng, S. Foelling, and M. Greiner, *Nature (London)* **462**, 74 (2009); J. Sherson, C. Weitenberg, M. Endres, M. Cheneau, I. Bloch, and S. Kuhr, *ibid.* **467**, 68 (2010).
 - [14] K. Eckert, O. Romero-Isart, M. Rodriguez, M. Lewenstein, E. S. Polzik, and A. Sanpera, *Nat. Phys.* **4**, 50 (2008).
 - [15] L. Santos, M. A. Baranov, J. I. Cirac, H.-U. Everts, H. Fehrmann, and M. Lewenstein, *Phys. Rev. Lett.* **93**, 030601 (2004).
 - [16] L. -M. Duan, E. Demler, and M. D. Lukin, *Phys. Rev. Lett.* **91**, 090402 (2003).
 - [17] A. B. Kuklov, and B. V. Svistunov, *Phys. Rev. Lett.* **90**, 100401 (2003).
 - [18] N. Marzari and D. Vanderbilt, *Phys. Rev. B* **56**, 12847 (1997).
 - [19] L. He and D. Vanderbilt, *Phys. Rev. Lett.* **86**, 5341 (2001).
 - [20] Z.-X. Chen, Z.-W. Zhou, X. Zhou, X.-F. Zhou, and G.-C. Guo, *Phys. Rev. A* **81**, 022303 (2010).
 - [21] R. Jordens, N. Strohmaier, K. Gunter, H. Moritz, T. Esslinger, *Nature (London)* **455**, 204 (2008).
 - [22] U. Schneider, L. Hackermuller, S. Will, Th. Best, I. Bloch, T. A. Costi, R. W. Helmes, D. Rasch, A. Rosch, *Science* **322**, 1520 (2008).
 - [23] L. De Leo, C. Kollath, A. Georges, M. Ferrero, O. Parcollet, *Phys. Rev. Lett.* **101**, 210403 (2008).
 - [24] R. Jordens, L. Tarruell, D. Greif, T. Uehlinger, N. Strohmaier, H. Moritz, T. Esslinger, L. De Leo, C. Kollath, A. Georges, V. Scarola, L. Pollet, E. Burovski, E. Kozik, and M. Troyer, *Phys. Rev. Lett.* **104**, 180401 (2010).
 - [25] A. H. Nevidomskyy, C. Scheiber, D. Senechal, and A.-M. S. Tremblay, *Phys. Rev. B* **77**, 064427 (2008).
 - [26] L. Capriotti and S. Sorella, *Phys. Rev. Lett.* **84**, 3173 (2000).
 - [27] R. R. P. Singh, Zheng Weihong, C. J. Hamer, and J. Oitmaa, *Phys. Rev. B* **60**, 7278 (1999).
 - [28] O. P. Sushkov, J. Oitmaa and Z. Weihong, *Phys. Rev. B* **63**, 104420 (2001).
 - [29] O. A. Starykh, R. R. P. Singh, and G. C. Levine, *Phys. Rev. Lett.* **88**, 167203 (2002).
 - [30] P. Sindzingre, J. B. Fouet, and C. Lhuillier, *Phys. Rev. B* **66**, 174424 (2002).
 - [31] G. De Chiara, O. Romero-Isart, and A. Sanpera, *Phys. Rev. A* **83**, 021604 (2011).
 - [32] Y. Chen, Z. D. Wang, F. C. Zhang, *Phys. Rev. B* **73**, 224414 (2006).